Electron-diffraction effects on scanning tunneling spectroscopy

Fredy R. Zypman
University of Puerto Rico, Department of Physics and Electronics, Humacao, Puerto Rico 00791-4300

Luis F. Fonseca
Department of Physics,University of Puerto Rico, Rio Piedras, Puerto Rico 00931-3343

(Received 1 December 1995; revised manuscript received 3 September 1996)

This paper provides further evidence for the relationship between density of states or local density of states (LDOS), and current-voltage (I-V) curves as obtained from scanning tunneling spectroscopy. A model that takes into account voltage-dependent wave functions is proposed. This model calculates both quantities and compares them. Current-carrying electrons are considered to come from the bulk of the tip and towards the tunneling region. From there, the electrons are diffracted back to the tip and forward into the sample. This scattering process is set within the framework of tight binding by providing boundary conditions. The method allows one to solve the steady-state problem, thus permitting the extraction of information even when the tip-sample distance is small (<1 Å). This is particularly important since it can probe regimes beyond the applicability of Bardeen approximation. For a tungsten tip and a silicon sample, the I-V curves closely follow the LDOS. On the other hand, the conductance-voltage curves present jumps that coincide with the Van Hove singularities of the semiconductor. [S0163-1829(97)07620-0]

I. INTRODUCTION

The high-spatial resolution of scanning tunneling microscopy (STM), combined with its intrinsic bias-dependent characteristics, makes it one of the most popular tools in surface physics.[1] The main open problem in scanning tunneling spectroscopy (STS) has been the inability to create clear-cut, general rules, between sought physical quantities and those that can be measured. All the efforts have concentrated in trying to find relationships between the density of states (DOS) or the local density of states (LDOS), and current-voltage (I-V) or conductance-voltage (σ-V) curves.[2–10] Experiments have been carried out on semiconductors,[11–13] superconductors,[14] and metals.[15] Arguments have been given[16,17] that support a correlation between DOS and σ-V curves for semiconductor samples. In the early times of STM, the Tersoff and Haman theory was able to explain some experimental results.[2] Concretely, STM images obtained at low bias and in the constant-current mode, represent constant-sample LDOS contours, LDOS being evaluated at the Fermi energy and at the center of the curvature of the tip. But, it is necessary to stress that this simple interpretation is no longer valid for high bias. Lang,[18] Selloni *et al.*,[19] Tsukada *et al.*,[20] Feenstra and Lutz,[21] and Zypman, Fonseca, and Goldstein[22] have extended the range of the theory to account for high bias voltages. Parallel to it, there have been models that specifically describe the behavior of the scanning tunneling microscope on metals.[23–25] Another problem with the theory of Tersoff and Hamman is the fact that it assumes a tip wave function with no angular dependence. The most common tips are made of tungsten or platinum-iridium. Those materials have, respectively, 85% and 98% of their electrons in d states. Therefore, it is reasonable to think that d states will contribute the most to the tunneling current. However, it has also been argued that atomic d states decay faster that s states and thus would not have as much an effect as otherwise expected. To resolve the matter, Chen has published a series of articles that provide a framework in which experimental results can be analyzed.[26–28] A common feature of most of these approaches is the use of Bardeen approximation,[29,30] a perturbative treatment of tunneling, to evaluate the electron transition probability between tip and sample. Basically, Bardeen's formula provides the interaction Hamiltonian between two, somewhat distant, systems. From that Hamiltonian, one can calculate the time-dependent tunneling transition rate between the systems. The popularity of this approximation lays in its simplicity and its consistency with experimental observations at large (albeit unspecified) tip-sample distances. However, the range of validity of the approximation remains undefined mainly because its applicability relies on the *qualitative* assumption that tip and sample interact weakly. There is no simple quantitative manner in which to calculate the strength of the interaction. A Green-function formalism based on Keldysh's theory of nonequilibrium processes[31] can be used to obtain a nonperturbative expression for the tunneling current. This approach has been useful to assess the accuracy of the Bardeen approximation.[32–35] Alternative approaches are required for dealing with ranges where the Bardeen approximation fails, and to define the ranges themselves. Since the typical tip-sample distances are of a few angstroms, it is not unreasonable to expect the formation of states with wave functions extending to both tip and sample, which will make the electron transfer from tip to sample a steady-state one. Under these conditions one can still talk of tunneling because the tip and the sample are two clearly defined and chemically distinct systems; this does not guarantee the applicability of the Bardeen formalism. In fact, the issue of resonant tunneling versus sequential tunneling to explain the mechanism of tunneling through quantum wells has been a subject of

debate.[36] In this paper we introduce a theoretical framework that makes no use of the Bardeen approximation and within which it is possible to calculate and compare steady-state characteristic curves (I-V, σ-V) and densities of states (DOS, LDOS; see Appendix B for definitions) even at high bias voltages. Also, the angular dependence of the wave function does not work against our results: first, because we are dealing here with spectroscopy, and the corrugation issues raised by the angular dependence have to do with topography; and second, because we use parameters so as to fit experimental energy bands without inquiring into the nature of the wave functions. Following our previous work,[22] in typical STM and STS conditions, that is, tip-sample voltage of few volts and tip-sample distance of 1–5 Å, it is expected that global tip-sample effects are of importance, and the behavior of the electron wave function between tip and sample does not have to be that of an evanescent exponential, but could have some richer structure. We model the tip and sample *as a whole system*. It consists of two cubes, one for the tip and one for the sample, linked by an atom (c atom, for channel atom) of the same chemical nature as the tip. Microscopically we assume that the cubes have simple cubic cell structure with different lattice constants. This assumption helps to simplify the computations, and we do not believe it will adversely affect our results. On the one hand, most of the tunneling current is determined by the position of the c atom, the remainder of the atoms serving basically as a reservoir of electrons. On the other hand, we want to check the resemblance between characteristic curves and densities of states on a *concrete* model sample.

We find the energies and wave function in the tight-binding (TB) approach. We consider, far away from the tunneling region, Bloch waves that are appropriate for this problem: an incoming wave towards the tunneling region, and a diffracted wave that consists of three parts, one purely reflected into the bulk, another spherically scattered into the bulk and, finally, a third one spherically diffracted forward into the sample. By choosing appropriate TB parameters we account for a metallic tip and a semiconductor sample. In the next section we present the general theory for this model and in the following section, we present concrete results for a case model.

These results show that I-V follows closely the LDOS of the sample at the Fermi energy evaluated at the position of the c atom. The σ-V curve presents a number of discontinuities at voltages that correspond to the Van Hove singularities of the DOS of the sample.

II. THEORY

Consider the tip-sample system (Fig. 1) to be the union of three regions. A semiconductor with simple cubic structure with N_S Wigner-Seitz cells on a side, a metal with simple cubic structure and N_T Wigner-Seitz cells on a side, and, inlaid between them, a c atom that serves as the channel for current between metal and semiconductor. The energy states are obtained in the near-neighbor TB approach[37] with an s-type basis function (cubium model[38]). This type of approach has been used in the past to study chemisorption on surfaces[38–40] and DOS of surface states.[41] Within this framework, the global wave function has the following expression in the tip and sample:[42]

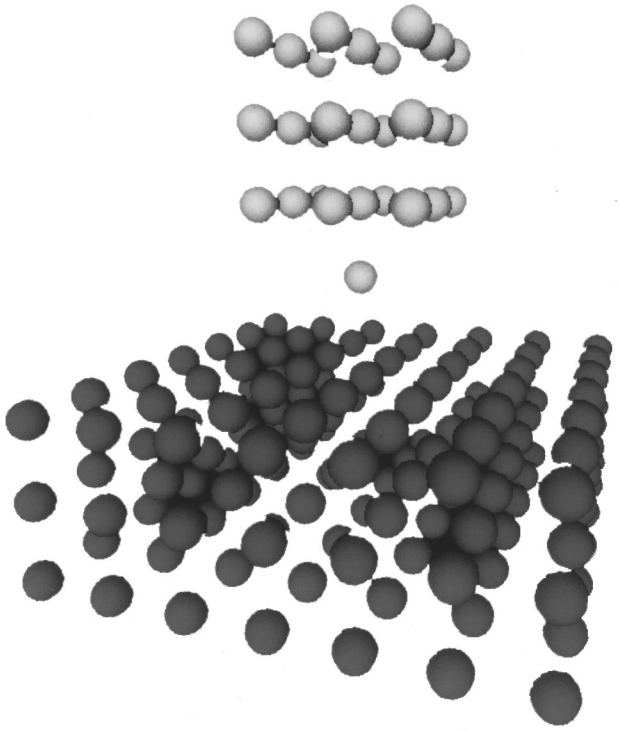

FIG. 1. Tip-sample system. The light gray spheres represent tungsten atoms and the dark gray spheres represent silicon atoms. Notice that the protruding c atom ''belongs'' to the tip.

$$\Psi_{\mathbf{k}}^{T}=\sum_{\mathbf{m}=\text{tip sites}} C_{\mathbf{m},\mathbf{k}}\Phi_{\mathbf{m}}, \tag{1}$$

$$\Psi_{\mathbf{K}}^{S}=\sum_{\mathbf{m}=\text{sample sites}} C_{\mathbf{m},K}\Phi_{\mathbf{m}} \tag{2}$$

where $\mathbf{k}$ is the tip electron-crystal momentum, K the sample crystal momentum, Φ_m are s-type atomic orbitals, and $C_{k,m}$ and $C_{K,m}$ are the expansion coefficients. The vector index $\mathbf{m}$ tags both tip and sample atomic sites, and can take $N_T^3+N_S^3+1$ different values. We impose, as the first boundary condition, that the wave function, far away from the c atom, be a Bloch wave:

$$C_{\boldsymbol{\theta},\mathbf{m}}\propto \mathbf{e}^{\pm i\mathbf{m}\cdot\boldsymbol{\theta}} \quad \text{for } |\mathbf{m}-\mathbf{m}_{c\ \text{atom}}|\geqslant m_0, \tag{3}$$

where m_0 is a number that gives an idea of the extent of the tunneling region. One expects it to be a single-digit number, because bulk properties are recovered a few atoms away from a perturbation to the perfect-crystal structure. In Eq. (3), θ is defined in the tip as $\mathbf{k}$ times the tip lattice constant, and in the sample as K times the sample-lattice constant. Concretely, in that far-away region, we take the sum of three terms for the tip wave function: an electron wave function with unit amplitude that comes from far away in the bulk; a specularly reflected electron wave function with amplitude $|B|^2$ that moves into the bulk, away from the tunneling region; and finally, a wave scattered from the c atom:

$$C^T = e^{i(m_x\theta_x^T + m_y\theta_y^T)}(e^{im_z\theta_z^T} + Be^{-im_z\theta_z^T}) + \frac{e^{im\theta}}{ma} f(\Omega_{\mathbf{m}}). \tag{4}$$

Here, $m=(m_x^2+m_y^2+m_z^2)^{1/2}$ is the distance to the origin in units of the appropriate lattice constant, and Ω_m is the solid angle in the direction of **m**.

For the sample, we consider a spherically scattered electron that moves away from the tunneling region, towards the sample bulk region,

$$C^s = \frac{e^{in\theta'}}{na_s} f(\Omega_{\mathbf{m}}). \tag{5}$$

It is important to stress that we do not assume any *a priori* form for the wave function in the region near the *c* atom. There are two ingredients that give rise to the form of Eqs. (4) and (5): starting backwards, the second ingredient is that the total wave function is a sum of an incident and a scattered wave. For the tip-sample system that we consider, the geometry is given by an atom (*c* atom) that separates a plane surface (the sample) from a very-large-radius-of-curvature tip. The tunneling is basically a localized phenomenon, the bulk of the tip and sample serving just as reservoirs of electrons. Thus, an electron approaching the tunneling region from the tip side will have two scattering components in the tip: one specularly reflected wave from the tip surface, and another decaying as the inverse of the distance from the *c* atom [Eq. (4)]. By the same token, the wave function in the sample of the same electron will consist only of a wave decaying as the inverse of the distance from the *c* atom [Eq. (5)].

The first ingredient is that in bulk (i.e., far away from any defect as impurities, surfaces, vacancies, etc.) the electron wave functions can be expanded in terms of Bloch waves [Eqs. (1)–(3)]. Notice that as we said in the previous paragraph, the coefficients C_{mk} in the tunneling region are not assumed to have any particular form. But, far away, the coefficients have a Bloch form [Eq. (3)].

As we mentioned above, these two ingredients allow us to write Eqs. (4) and (5). The last ingredient provides the global behavior of the wave function. The first one gives the local behavior (locally, in the far-away region, the decaying wave becomes a Bloch wave, the decaying, 1/ma, term being absorbed in the amplitude). In fact, Eqs. (4) and (5) are a subset of those of the form given by Eq. (3). By choosing these particular forms we are actually imposing the boundary conditions needed to solve the Schrödinger equation.

In the tunneling region, the TB coefficients will be found solving the appropriate TB equations as shown below. The energy of the whole system is parametrized like in bulk as

$$\begin{aligned} E &= \alpha^T + 2\beta^T(\cos\theta_x^T + \cos\theta_y^T + \cos\theta_z^T) \\ &= eV + \alpha^s + 2\beta^s(\cos\theta_x^s + \cos\theta_y^s\ \cos\theta_z^s), \end{aligned} \tag{6}$$

where V is the voltage applied between the tip and the sample and e is the charge of the electron. α is the Coulomb integral and β the resonance integral.

In order to obtain the current we need to evaluate $f(\Omega_m)$ for the sample (along the way, we will get all the coefficients C_m). The basic TB problem is to solve the Schrödinger equation as an eigenvalue problem,

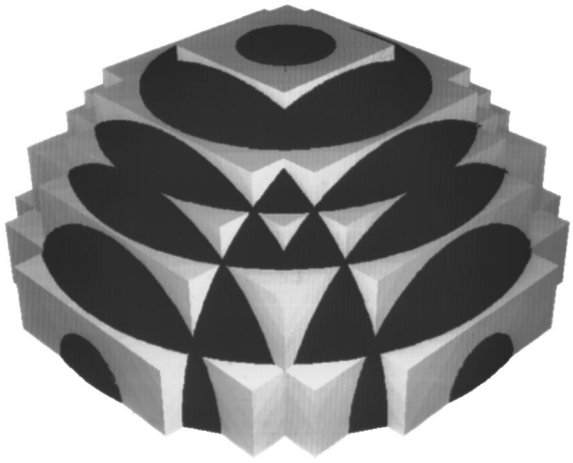

FIG. 2. View of the top side of the tetris (light gray) and the embedded sphere (dark gray) that it approximates.

$$T\cdot\mathbf{C} = E\mathbf{C}, \tag{7}$$

where **C** is the vector of the TB coefficients at sites **m**, T is the TB matrix that has, as matrix elements $(\mathbf{m},\mathbf{m}')$, the appropriate Coulomb and resonance integrals between sites **m** and $\mathbf{m}'$. In the case we are considering here, the energies $E=E(\theta)$ are given in Eq. (6) since the solutions to Eq. (7) are those of bulk far from the interfaces. In order to separate the tunneling region from the far region, we considered a sphere with large radii as compared with the lattice constant. The points inside the sphere belong, by definition, to the tunneling region. Those that lie outside belong to the far region.

The coefficients [Eqs. (1) and (2)] of the wave functions are defined not in a continuum, but in a discrete space. This space is spanned by the lattice sites. The tetris is the best approximation of the sphere in the discrete space. The corners of the tetris are properly assigned wave-function coefficients. In this way the tetris represents the discrete surface on which we impose our boundary conditions.

Figure 2 provides visual insight into the nature of the approximation. Figure 3 helps to better understand the geometry of the different regions, that is, tunneling, far, and boundary. In the inset there are four atoms that can be seen to belong roughly to the same solid angle. Figure 4 shows that three of them are on the surface of the tetris, and are bona fide points of our problem (because in our problem we only explicitly deal with points inside and on the tetris). The fourth one on the top right is not. In order to keep our unknowns from proliferating we resorted to the trick described in Appendix A. To find **C**, we construct a tetris surface as described above. We take the radius of the tetris to be larger than m_0 from Eq. (3). That guarantees that, on the tetris and outside it, the C_m are given by Eq. (4) or (5), with B and $f(\Omega_m)$ still unknown. Next, consider those sites just outside the tetris, that are near neighbors to the atoms on the tetris. The corresponding coefficients also are bulk type, and can be written back in terms of the coefficients on the tetris by using Eq. (4) or (5). This means that we are able to add new equations (which are actually boundary conditions) without adding new variables. It is important to notice that among those equations, there are some that are inhomoge-

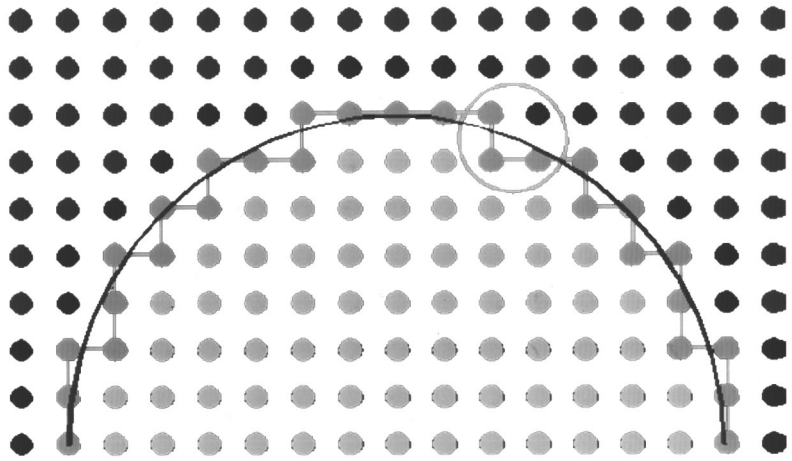

FIG. 3. Cross section of Fig. 2.

neous, coming from the term $e^{\mathrm{im}\theta}$ on the tip side. Let $\mathbf{v}=\{v_m\}$ be the vector of inhomogeneous terms, which has nonzero components for **m** belonging on the tetris on the tip side. Equation (7) can now be written (see Appendix A)

$$(T-E_{\boldsymbol{\theta}})\cdot\mathbf{C}_{\boldsymbol{\theta}}=\mathbf{v}_{\boldsymbol{\theta}} \tag{8}$$

or

$$\mathbf{C}_{\boldsymbol{\theta}}=\frac{1}{T-E_{\boldsymbol{\theta}}}\cdot\mathbf{v}_{\boldsymbol{\theta}}\,, \tag{9}$$

which provides the TB coefficients. In particular, Eq. (9) provides the coefficients of the sample on the tetris and, from Eq. (5),

$$f(\Omega_{\mathbf{m}})=ma_s e^{-\mathrm{im}\theta^s}C_{\mathbf{m},\boldsymbol{\theta}^T}\,, \tag{10}$$

where θ^s is a function of θ^T according to Eq. (6).

To evaluate *I-V*, we start by writing the current density as[43]

$$\mathbf{J}_{\boldsymbol{\theta}^T}=J_{\boldsymbol{\theta}^T}\mathbf{e}_r=\frac{e\hbar\,\theta^s}{a_s m_e r^2}\,|f_{\boldsymbol{\theta}^T}|^2\mathbf{e}_r\,, \tag{11}$$

and the current for a state θ^T is

$$I_{\boldsymbol{\theta}^T}=\frac{e\hbar\,\theta^s}{a_s m_e}\int_{\text{tetris}}\frac{1}{r^2}\,|f_{\boldsymbol{\theta}^T}|^2 r^2 d\Omega$$

$$=\frac{e\hbar\,\theta^s}{a_s m_e}\sum_{\mathbf{m}\in(\text{tetris samples})}|f_{\boldsymbol{\theta}^T}|^2\Delta\Omega_{\mathbf{m}}\,. \tag{12}$$

Finally, the total current is the sum of all the contributions from states θ_T with energies below the Fermi energy:

$$I=\sum_{\boldsymbol{\theta}_T:E(\boldsymbol{\theta}_T)<E_F}I_{\boldsymbol{\theta}_T}\,. \tag{13}$$

III. APPLICATION TO A W TIP AND Si SAMPLE

In this section we apply the general results obtained in Sec. II to the particular and common case in which a tungsten tip is used to investigate a silicon sample. It is important to notice that these materials are considered within the constraints of the model we are using and, therefore, the TB parameters used serve to fit the energy of the middle of the band and its width for silicon, and the bottom of the band and its curvature for tungsten. It does not provide the full band structure. This is enough for our purposes though, because we want to compare currents and densities of states

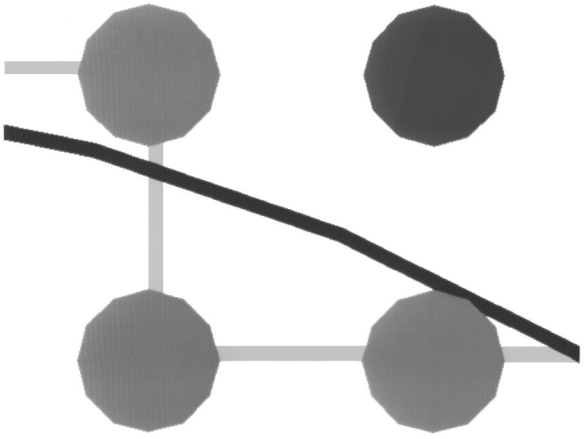

FIG. 4. Zoom of the inset in Fig. 3. We consider the tight-binding wave function in the tetris surface to be that of a diffracted electron. All the atom sites in this figure are located in almost the same solid angle measured from the *c* atom.

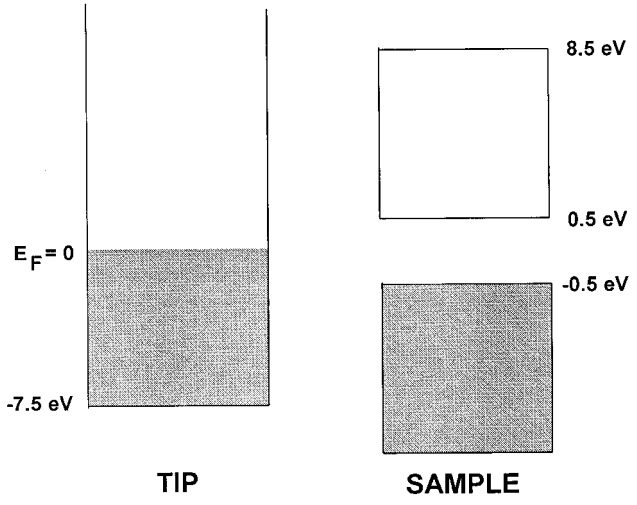

FIG. 5. Energy-level diagram for the tip-sample system at zero bias voltage. As the voltage is raised, the tip levels move up.

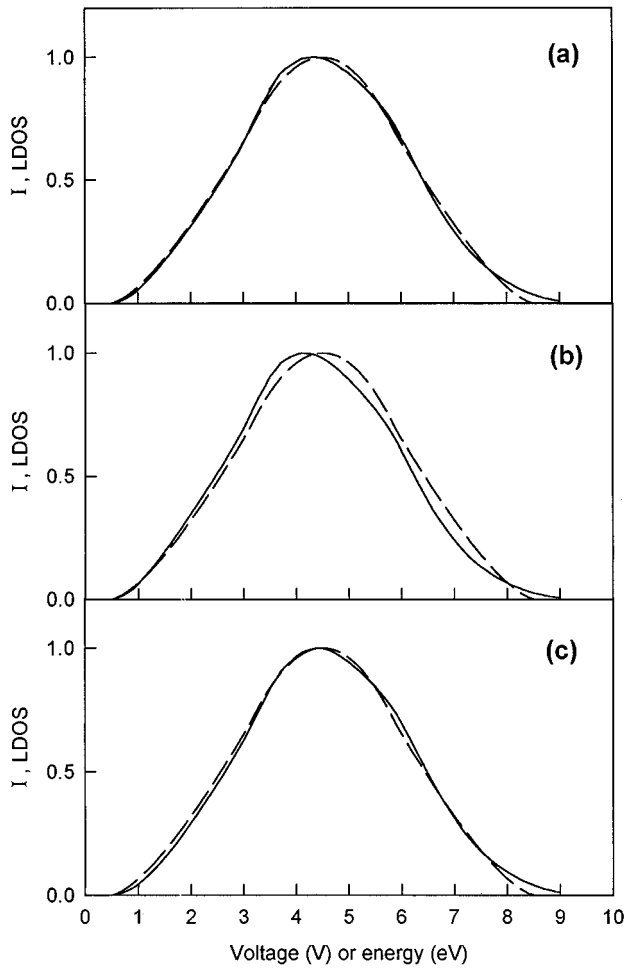

FIG. 6. Normalized tunneling current I (continuous curve) and LDOS (dashed) as a function of voltage or energy, respectively, for the following tip-sample separations: (a) 5 Å, (b) 3 Å, and (c) 1 Å. The zero of the energy is located at the middle of the band gap of the sample.

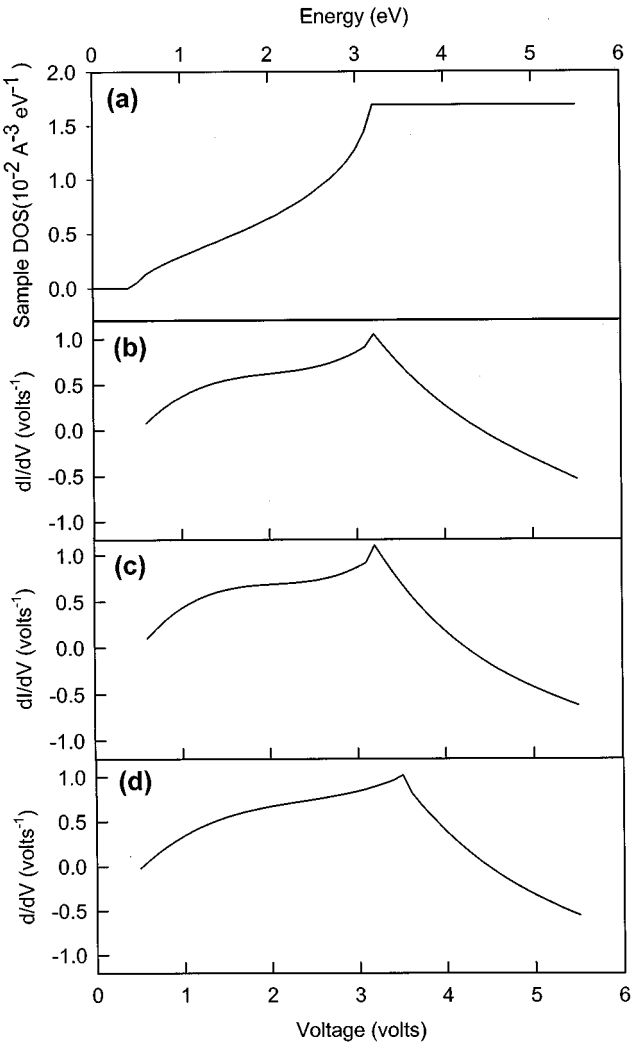

FIG. 7. dI/dV vs voltage for various tip-sample separations. Breaks in the function can be seen at about 3.5 and 6.0 eV, which correspond to the Van Hove singularities of the sample; (b) 5 Å, (c) 3 Å, and (d) 1 Å. For comparison, (a) gives the DOS of the sample showing the Van Hove singularities.

self-consistently, *within the same model*. In order to obtain the proper conduction band for Si (the band gap of 1 eV is artificially obtained by locating the Fermi energy 0.5 eV below the bottom of the conduction band), and the Fermi energy for W, we take $\alpha_s = -9$ eV, $\beta_s = 0.67$ eV, $E_F = -13.5$ eV, the minimum energy of the tip is located at -19.5 eV. Figure 5 shows the energy-level diagram assigning $E_F = 0$ eV. In the tunneling region, we assume that the c atom interacts with tip, and sample through the proper resonance integrals as $\beta_{c-T} = 3.5$ eV, $\beta_{c-s} = 41\,537.63\, d^4 e^{-5.358d}$ where d is the separation between the c atom and the sample surface, and β is in eV and d in Å (Refs. 44–46) (the decay lengths of tip and sample are 0.4 and 0.35 Å, respectively). With these parameters we investigated various features of the system. First, we want to know to what extent does $I(V)$ follow the sample LDOS. Figure 6 shows I-V and LDOS for tip-sample separations of 1, 3, and 5 Å. We can see that the two curves have a closer resemblance and therefore, the STM I-V curve is a good measure of the LDOS roughly for separations of 1–5 Å. This result is in agreement with work on metals,[13,47] at low voltages in general,[2] and with similar works.[48,49]

A second question we address here is what are the states that contribute most to the current. For that purpose, we calculated (for $d = 1$, 3, and 5 Å), the I-V due to all states, and the I-V produced by a narrow band (less than 0.1 eV) below E_F. We found that both results agree within 1% and therefore, the current is coming mostly from states with energies close to E_F.

Finally, we use our model to study the relationship between density of states and dI/dV. This is important since it has been argued that it is this quantity, and not I-V that is relevant.[17] Figure 7 shows dI/dV curves for tip-sample separations of 1, 3, and 5 Å. The most interesting feature is that it presents nondifferentiable points that correspond to the Van Hove singularities of the DOS of the sample. Concretely, we see a jump of dI/dV at 3.5 V, which comes from the Van Hove singularity of Si. The jump is not extremely sharp because as the voltage varies, a few tip states close to E_F contribute to the current.

IV. CONCLUSIONS

We have presented a method for calculating steady-state tunneling current in STM by using running Bloch functions. We have used the method to study the common experimental situation of a tungsten tip and a silicon sample. Results show that I-V curves follow the sample LDOS. Our model provides a good tool to investigate resonant tunneling that is more important in the small distances regime.

Our results also prove that most of the tunneling current comes from states with energies close to the Fermi energy.

In agreement with previous work,[22] we found that dI/dV present nondifferentiable points that come from the Van Hove singularities of the sample.

Finally, from an experimental point of view, we provide a framework within which more experimental results can be interpreted. The method introduced here can be applied to a wide variety of materials and situations.

ACKNOWLEDGMENTS

This work was supported by NSF Grant No. OSR-9452893 (L.F.F. and F.R.Z.) and Grant No. NIH GM-08216 (F.R.Z.).

APPENDIX A

Here we present an example on how the TB equations are built. In particular, we show how the inhomogeneous term appears. Let us, for example, consider the equation corresponding to the site located in the center of the top plane of the tetris. For the tip sites, far from the c atom, we have

$$C_{\mathbf{n}}=e^{i(n_x\theta_x+n_y\theta_y)}(e^{\mathrm{in}_z\theta_z}+Be^{-\mathrm{in}_z\theta_z})+\frac{e^{\mathrm{in}\theta}}{na}f(\Omega). \quad \text{(A1)}$$

Let us say that the site we are considering is located at $\mathbf{n}=\mathbf{n}_0$. Its near neighbors are, one on top ($\mathbf{n}=\mathbf{n}_\uparrow$, a bulk site), one below ($\mathbf{n}=\mathbf{n}_\downarrow$, a tunneling region site), and four on the top plane, in front ($\mathbf{n}_F$), back ($\mathbf{n}_B$), right ($\mathbf{n}_R$) and left ($\mathbf{n}_L$) boundary sites.

The basic TB equation for the site $\mathbf{n}_0$ is

$$[\alpha-E]C_{n_0}+\beta[C_{n_\uparrow}+C_{n_\uparrow}+C_{n_F}+C_{n_B}+C_{n_R}+C_{n_L}]=0. \quad \text{(A2)}$$

All the C's are *a priori*, unknown, but to avoid proliferation of unknowns (and be able to solve the Schrödinger system) we ''fold back'' all the external coefficients (in this equation only $C_{n_\uparrow}$) into the ''internal'' ones. To do that, we notice that the site $\mathbf{n}_0$, and the site $\mathbf{n}_\uparrow$ are both at the same angular location (measured from the c atom) and then, the scattering amplitude $f(\Omega)$ (which only depends on the angle, not distance) is the same for both. So,

$$C_{\mathbf{n}_0}=e^{i(n_{0x}\theta_x+n_{0y}\theta_y)}(e^{\mathrm{in}_{0z}\theta_z}+Be^{-\mathrm{in}_{0z}\theta_z})+\frac{e^{\mathrm{in}_0\theta}}{n_0a}f(\Omega), \quad \text{(A3)}$$

$$C_{\mathbf{n}_\uparrow}=e^{i(n_{\uparrow x}\theta_x+n_{\uparrow y}\theta_y)}(e^{\mathrm{in}_{\uparrow z}\theta_z}+Be^{-\mathrm{in}_{\uparrow z}\theta_z})+\frac{e^{\mathrm{in}_\uparrow\theta}}{n_\uparrow a}f(\Omega). \quad \text{(A4)}$$

By eliminating $f(\Omega)$ from both equations, we can write $C_{n_\uparrow}$ in terms of C_{n_0} as:

$$\begin{aligned}C_{\mathbf{n}_\uparrow}=&e^{i(n_{\uparrow x}\theta_x+n_{\uparrow y}\theta_y)}(e^{\mathrm{in}_{\uparrow z}\theta_z}Be^{-\mathrm{in}_{\uparrow z}e_z})\\&+\frac{e^{\mathrm{in}_\uparrow\theta}}{n_\uparrow}[C_{\mathbf{n}_0}-e^{i(n_{0x}\theta_x+n_{0y}\theta_y)}\\&\times(e^{\mathrm{in}_{0z}\theta_z}+Be^{-\mathrm{in}_{0z}\theta_z})]e^{-\mathrm{in}_0\theta}n_0. \quad \text{(A5)}\end{aligned}$$

Substituting in Eq. (A2)

$$\begin{aligned}&\left(\alpha-E+\beta\frac{n_0}{n_\uparrow}e^{i(n_\uparrow-n_0)}\right)C_{\mathbf{n}_0}+\beta\left[e^{i(n_{\uparrow x}\theta_x+n_{\uparrow y}\theta_y-n_{\uparrow z}\theta_z)}\right.\\&\left.-\frac{n_0e^{i(n_\uparrow-n_0)}}{n_\uparrow}e^{i(n_{0x}\theta_x+n_{0y}\theta_y-n_{0z}\theta_z)}\right]B+\beta C_{n_\downarrow}+\beta C_{n_F}\\&+\beta C_{n_B}+\beta C_{n_R}+\beta C_{n_L}\\&=\beta\left[\frac{n_0}{n_\uparrow}e^{i(n_\uparrow-n_0)\theta}e^{i\mathbf{n}_0\cdot\boldsymbol{\theta}}-e^{in_\uparrow\theta}\right]. \quad \text{(A6)}\end{aligned}$$

So we can see how this equation on the C_S and B is inhomogeneous. Also from the process we can see why equations for sites *inside* the tetris are homogeneous.

APPENDIX B

In this appendix we present definitions for DOS and LDOS as used in this paper.

The LDOS of a system at a given location and for a given energy is defined as the number of states per unit energy times the probability that the electron be at the given location. While the local density of states is

$$D(E_0)=A\sum_{\theta:E(\theta)=E_0}1, \quad \text{(B1)}$$

the LDOS is

$$L(E_0)=A\sum_{\theta:E(\theta)=E_0}|\Psi|^2_{\text{sample at tip's position}}, \quad \text{(B2)}$$

where A is a constant.

From Eq. (2) in the paper,

$$L(E_0)=\sum_{\theta,E(\theta)=E_0}\left|\sum_{\mathbf{m}}C_{\mathbf{m},\boldsymbol{\theta}}\Phi_{\mathbf{m}}\right|^2 \quad \text{(B3)}$$

and, with the same approximations used in Ref. 22,

$$L=\text{const}\sum_{\theta_1,\theta_2,\theta_3}\sum_{\theta_2',\theta_2',\theta_3'}|C_{SH}|^2e^{-2r/a_s(V)}, \quad \text{(B4)}$$

where const is a normalization constant, C_{SH} is the TB coefficient of the sample at the ''host'' atom, that is, the closest to the c atom. Finally, the decay rate of the sample amplitude as a function of applied voltage is

$$a_s(V)=\frac{0.35\ \text{Å}}{\sqrt{1+(0.35\ \text{Å})^2(2me/\hbar^2)V}}. \quad \text{(B5)}$$

[1] R. Wiesendanger, *Scanning Probe Microscopy and Spectroscopy* (Cambridge University Press, Cambridge, 1994).
[2] J. Tersoff and D. R. Hamann, Phys. Rev. B **31**, 805 (1985).
[3] N. D. Lang, Phys. Rev. Lett. **55**, 230 (1985).
[4] N. D. Lang, Phys. Rev. Lett. **55**, 2925 (1985).
[5] C. J. Chen, J. Vac. Sci. Technol. A **6**, 319 (1988).
[6] C. R. Leavens and G. C. Aers, Phys. Rev. B **38**, 7357 (1988).
[7] E. Tekman and S. Ciraci, Phys. Rev. B **40**, 10 286 (1989).
[8] S. Ciraci and E. Tekman, Phys. Rev. B **40**, 11 969 (1989).
[9] C. J. Chen, Phys. Rev. Lett. **65**, 448 (1990).
[10] G. Doyen, D. Drakova, and M. Scheffler, Phys. Rev. B **47**, 9778 (1993).
[11] R. M. Feenstra, J. Vac. Sci. Technol. B **7**, 925 (1989).
[12] P. Avouris and I. Lyo, Surf. Sci. **242**, 1 (1991).
[13] R. J. Hamers, R. M. Tromp, and J. E. Demuth, Phys. Rev. Lett. **56**, 1972 (1986).
[14] H. F. Hess, R. B. Robinson, R. C. Dynes, J. M. Valles, Jr., and J. V. Waszczak, J. Vac. Sci. Technol. A **8**, 450 (1990).
[15] L. C. Davis, M. P. Everson, R. C. Jaklevic, and W. Shen, Phys. Rev. B **43**, 3821 (1991).
[16] J. A. Stroscio, R. M. Feenstra, and A. P. Fein, Phys. Rev. Lett. **57**, 2579 (1986).
[17] R. M. Feenstra, J. A. Stroscio, and A. P. Fein, Surf. Sci. **181**, 295 (1987).
[18] N. D. Lang, Phys. Rev. B **34**, 5947 (1986).
[19] A. Selloni, P. Carnevalli, E. Tosati, and C. D. Chen, Phys. Rev. B **31**, 2602 (1985).
[20] M. Tsukada, K. Kobayashi, N. Isshiki, and H. Kageshima, Surf. Sci. Rep. **13**, 2 (1991).
[21] R. M. Feenstra and M. A. Lutz, Phys. Rev. B **42**, 5391 (1990).
[22] F. R. Zypman, L. F. Fonseca, and Y. Goldstein, Phys. Rev. B **49**, 1981 (1994); F. R. Zypman and L. F. Fonseca, *ibid*. **51**, 2501 (1995).
[23] R. Tromp, J. Phys. Condens. Matter **1**, 10 211 (1989).
[24] R. J. Hamers, in *Scanning Tunneling Microscopy I*, edited by H. J. Güntherodt and R. Wiesendanger, Springer Series in Surface Sciences Vol. 20 (Springer, New York, 1992).
[25] R. J. Hamers, Annu. Rev. Phys. Chem. **40**, 531 (1989).
[26] C. J. Chen, Phys. Rev. B **42**, 8841 (1990).
[27] C. J. Chen, Phys. Rev. Lett. **65**, 448 (1990).
[28] C. J. Chen, J. Vac. Sci. Technol. A **9**, 44 (1991).
[29] J. Bardeen, Phys. Rev. Lett. **6**, 57 (1961).
[30] A. A. Lucas, Europhys. News **21**, 63 (1990).
[31] L. V. Keldysh Zh. Eksp. Teor. Fiz. **47**, 1945 (1964) [Sov. Phys. JETP **20**, 1018 (1965)].
[32] A. A. Lucas, H. Morawitz, G. R. Henry, J. P. Vigneron, Ph. Lambin, P. H. Cutler, and T. E. Feuchtwang, Phys. Rev. B **37**, 10 708 (1988).
[33] C. Noguera, J. Microsc. **152**, 3 (1988).
[34] C. Noguera, J. Phys. **50**, 2587 (1989).
[35] C. Noguera, Phys. Rev. B **42**, 1629 (1990).
[36] S. Luryi, Appl. Phys. Lett. **47**, 490 (1985).
[37] N. F. Mott and H. Jones, *The Theory of the Properties of Metals and Alloys* (Dover, New York, 1958).
[38] T. L. Einstein, Surf. Sci. **45**, 713 (1974).
[39] T. L. Einstein, Phys. Rev. B **12**, 1262 (1975).
[40] T. L. Einstein and J. R. Schrieffer, Phys. Rev. B **7**, 3629 (1973).
[41] D. Kalkstein and P. Soven, Surf. Sci. **26**, 85 (1971).
[42] T. B. Grimley, J. Phys. Chem. Solids **14**, 227 (1960).
[43] C. Cohen-Tannoudji, B. Diu, and F. Laloë, *Quantum Mechanics* (Wiley, New York, 1977), Vol. 2.
[44] J. R. Smith, T. Perry, A. Banerjea, J. Ferrante, and G. Bozzolo, Phys. Rev. B **44**, 6444 (1991).
[45] M. Posternak, H. Krakauer, A. J. Freeman, and D. D. Koelling, Phys. Rev. B **21**, 5601 (1980).
[46] J. A. Applebaum and D. R. Hamann, Phys. Rev. Lett. **31**, 106 (1973).
[47] R. S. Becker, J. A. Golovchenko, D. R. Hamann, and B. S. Swartzentruber, Phys. Rev. Lett. **55**, 2032 (1985).
[48] J. Ferrer, A. Martin-Rodero, and F. Flores, Phys. Rev. B **38**, 10 113 (1988).
[49] W. Sacks and C. Nogera, Phys. Rev. B **43**, 11 612 (1991).